

## Stabilization of the lattice Boltzmann method by the $H$ theorem: A numerical test

Santosh Ansumali and Iliya V. Karlin\*

*ETH-Zürich, Department of Materials, Institute of Polymers, ETH-Zentrum, Sonneggstrasse 3, ML J 27, CH-8092 Zürich, Switzerland*

(Received 7 June 2000)

For a one-dimensional benchmark shock tube problem, we implement the lattice Boltzmann method based on the  $H$  theorem [I. Karlin, A. Ferrante, and H. C. Öttinger, *Europhys. Lett.* **47**, 182 (1999)]. Results of simulation demonstrate significant improvement of stability, as compared to realizations without explicit entropic estimations.

PACS number(s): 47.11.+j, 05.20.Dd

### I. INTRODUCTION

Since the invention of the lattice-gas model [1], lattice-based methods for simulations of complex hydrodynamic phenomena received much attention over the past decade. In these methods, hydrodynamic equations are not addressed by a direct discretization procedure, rather, a simple pseudoparticle kinetics is introduced in such a way that the hydrodynamic equations are obtained on the large space and time scale. Particularly promising is the well-known lattice Boltzmann method (LBM) [2]. It is based on the fully discrete velocity-space-time kinetic equation of the form,

$$N(x+c, t+1) - N(x, t) = \Delta[N(x, t)]. \quad (1)$$

Here  $N(x, t)$  is the  $b$ -component vector of populations  $N_i$  of the pseudoparticles with velocities  $c_i$ , at the sites  $x$  of a lattice at discrete time  $t$ . The system of discrete velocities at any site is formed by the outgoing links of the lattice, and it also may include the zero vector.

One of the most important problems related to the LBM, recognized by many authors, is the problem of numerical stability. For the LBM related to incompressible flow simulations, numerical instabilities preclude so far a study of high Reynolds number flow situations. Instabilities become even more annoying for compressible flows [3].

It has been discussed for some time in the literature that stability of the LBM could be improved if the method could be equipped with an analog of the Boltzmann  $H$  theorem. Recently, theoretical progress in this direction has been achieved [4–8]. In particular, for the isothermal LBM, the hydrodynamic fields are the density,  $\rho = (\mathbf{1}, N)$ , and the average momentum,  $\rho u_\alpha = (c_\alpha, N)$ , where  $(\cdot, \cdot)$  denotes the standard scalar product in the  $b$ -dimensional space of population vectors. In this case, one can construct entropy functions in such a way that its local equilibrium implies the crucial relation for the stress tensor,

$$(c_\alpha c_\beta, N^{\text{eq}}) = c_s^2 \rho \delta_{\alpha\beta} + \rho u_\alpha u_\beta,$$

up to the admissible degree of accuracy of the LBM [6]. Furthermore, it has been suggested how to construct the col-

lision integral  $\Delta$  based solely on the knowledge of the entropy function, and how to stabilize the updates on the basis of the discrete-time  $H$  theorem [6,8]. In the sequel, we term the LBM based on the  $H$  theorem the entropic lattice Boltzmann method (ELBM).

It is the goal of this paper to test the aforementioned theoretical developments for a shock tube problem. This one-dimensional benchmark problem has been suggested some time ago [9] for testing various ideas in the LBM. Though this model is based on a very simple three-velocity lattice, it provides a stringent test of stability. Implementation of the ELBM demonstrated a large improvement of stability in this benchmark problem. In fact, we were able to reach the values of the kinematic viscosity as low as  $10^{-12}$  without any sign of numerical instabilities. The most important part of the realization is a robust root-finding procedure which implements the  $H$  theorem.

### II. CONSTRUCTION OF THE ELBM

An advantage of the LBM in comparison to the lattice-gas method is that the Galilean invariance of the Navier-Stokes equation is easier to control in the former than in the latter. In order that this advantage should not get lost in the ELBM, entropy functions should be found for each lattice separately. We here consider the one-dimensional lattice with spacing  $c$ , and the population vector at each site  $x$  has three components,  $N = (N_+, N_0, N_-)^\dagger$ , corresponding to velocities  $c_+ = c$ ,  $c_0 = 0$ , and  $c_- = -c$ , respectively. For this model, the entropy function has been found in [6]

$$H = N_0 \ln(N_0/4) + N_- \ln(N_-) + N_+ \ln(N_+). \quad (2)$$

Realizations of the ELBM based on the entropy function (2) result in the one-dimensional Navier-Stokes equation with the sound speed  $c_s = \sqrt{1/3}c$ , within the accuracy of the order  $(u/c_s)^4$ . Construction of the ELBM involves the following two steps (these steps are independent of the choice of the entropy).

First, we specify bare collision integral  $\Delta$  in such a way as to satisfy the admissibility condition,  $(\Delta, \mathbf{1}) = (\Delta, c_\alpha) = 0$ ,  $(\Delta, \nabla H) \leq 0$ , and  $\Delta(N^{\text{eq}}) = 0$ . Here  $\nabla H$  is the gradient of  $H$  in the space of population vectors. The choice of the bare collision integral is not unique. We here consider three cases,

$$\Delta = (g^+ - g^-) \{ \exp[(\nabla H, g^-)] - \exp[(\nabla H, g^+)] \}, \quad (3a)$$

\*Corresponding author. FAX: +41 01 632 10 76. Email address: [ikarlin@ifp.mat.ethz.ch](mailto:ikarlin@ifp.mat.ethz.ch)

$$\mathbf{\Delta} = (\mathbf{g}^+ - \mathbf{g}^-)(\nabla H, \mathbf{g}^- - \mathbf{g}^+), \quad (3b)$$

$$\mathbf{\Delta} = N^{\text{eq}}(\mathbf{N}) - \mathbf{N}, \quad (3c)$$

where  $\mathbf{g}^+ = (1, 0, 1)^\dagger$ , and  $\mathbf{g}^- = (0, 2, 0)^\dagger$  are positive and negative parts of the vector  $\mathbf{g} = \mathbf{g}^+ - \mathbf{g}^-$ , the latter is orthogonal to the vectors of conserved fields,  $(\mathbf{g}, \mathbf{1}) = 0$ , and  $(\mathbf{g}, \mathbf{c}) = 0$ . Collision integral of the form (3a) has been suggested in Ref. [6], and is motivated by well-known models of chemical kinetics in the framework of so-called Marcelin-De Donder kinetic function [10]. Collision integral (3b) is a linearized form thereof, and it is motivated by recently introduced GENERIC models of nonequilibrium thermodynamics [11]. Equation (3c) is the familiar Bhatnagar-Gross-Krook (BGK) form.

Second, the population vector is updated according to the kinetic equation

$$N(x + \mathbf{c}, t + 1) - N(x, t) = \mathbf{\Delta}^*[N(x, t)], \quad (4)$$

where  $\mathbf{\Delta}^*$  is a *dressed* (or *stabilized*) collision integral,

$$\mathbf{\Delta}^*[N(x, t)] = \beta \alpha[N(x, t)] \mathbf{\Delta}[N(x, t)]. \quad (5)$$

Here  $\beta \in [0, 1]$  is a parameter related to viscosity [see Eq. (20) below], and  $\alpha$  is the scalar function of the population vector. Function  $\alpha$  ensures the discrete-time  $H$  theorem, and is the nontrivial root of the scalar nonlinear equation,

$$H(N) = H(N + \alpha \mathbf{\Delta}[N]). \quad (6)$$

Put differently, bare collision integrals are stripped of any relaxation time parameters, and are merely directions in the space of populations, pointing towards the change of the state in the collision event. Parameter  $\alpha$  defines the maximal admissible collision step along this direction so that the entropy will not decrease. The combination  $\beta \alpha$  is thus the effective relaxation time in the fully discrete kinetic picture.

An advantage of the bare BGK collision integral in the ELBM scheme is not obvious: In most cases, the local equilibrium is not known as an explicit function of the hydrodynamic fields, and has to be evaluated numerically on each iteration of the method for each lattice cite. However, after the local equilibrium is found, the resulting bare BGK collision integral must be dressed by numerically solving Eq. (6). Thus, in comparison to bare collision integrals (3a) and (3b) which only require the knowledge of the entropy but not of the local equilibrium, numerical efforts roughly double. In the example considered here we were able to find analytically the local equilibrium of the  $H$  function (2),

$$\begin{aligned} N_0 &= \frac{2\rho}{3} [2 - \sqrt{1 + M^2}], \\ N_+ &= \frac{\rho}{3} \left[ \frac{uc - c_s^2}{2c_s^2} + \sqrt{1 + M^2} \right], \\ N_- &= \frac{\rho}{3} \left[ -\frac{uc + c_s^2}{2c_s^2} + \sqrt{1 + M^2} \right], \end{aligned} \quad (7)$$

where  $M^2 = u^2/c_s^2$  is the Mach number squared. However, result (7) is the exclusive case which does not happen in higher dimensions.

### III. IDENTIFICATION OF VISCOSITY

Identification of the viscosity coefficient in the ELBM is done on the basis of the Chapman-Enskog analysis [12] in the vicinity of the local equilibrium, in the same way as in the standard lattice Boltzmann realizations. Let us do this derivation in some detail for the example given here.

Linearization of the dressed collision integral (5) may be written as

$$\delta \mathbf{\Delta}^* = \beta \alpha(N^{\text{eq}}) (\nabla \mathbf{\Delta}|_{N^{\text{eq}}, \delta N}) + \beta (\nabla \alpha|_{N^{\text{eq}}, \delta N}) \mathbf{\Delta}(N^{\text{eq}}). \quad (8)$$

The last term on the right-hand side of the latter expression is equal to zero by the construction of the bare collision integral. In the sequel, we denote as  $\mathbf{L}$  the matrix of the derivatives of the bare collision integral at the local equilibrium, and write  $\alpha_{\text{eq}} = \alpha(N^{\text{eq}})$ ,

$$\delta \mathbf{\Delta}^* = \beta \alpha(N^{\text{eq}}) \mathbf{L} \delta N. \quad (9)$$

For the bare collision integrals (3a) and (3b), the components of the matrix  $\mathbf{L}$  have the form

$$L_{ij} = -K_{\text{eq}} g_i \sum_k \frac{\partial^2 H}{\partial N_j \partial N_k} \Big|_{N^{\text{eq}}} g_k, \quad (10)$$

where positive scalar functions  $K_{\text{eq}}$  are  $K_{\text{eq}} = \exp[(\nabla H|_{N^{\text{eq}}, \mathbf{g}^\pm})]$  and  $K_{\text{eq}} = 1$  for the collision integrals (3a) and (3b), respectively. Function  $\alpha_{\text{eq}}$  is found upon expanding Eq. (6) at equilibrium up to the quadratic in  $\delta N$  terms. [Note that a substitution of  $N^{\text{eq}}$  into Eq. (6) does not give an equation for  $\alpha_{\text{eq}}$ ]. This results in the following quadratic equation:

$$\begin{aligned} \alpha_{\text{eq}} \left( \frac{1}{2} \alpha_{\text{eq}} \sum_{ijk} \delta N_i \frac{\partial^2 H}{\partial N_i \partial N_j} \Big|_{N^{\text{eq}}} L_{jk} \delta N_k \right. \\ \left. + \sum_{ijkl} L_{ij} \delta N_j \frac{\partial^2 H}{\partial N_i \partial N_k} \Big|_{N^{\text{eq}}} L_{kl} \delta N_l \right) = 0. \end{aligned} \quad (11)$$

For the bare BGK collision integral (3c), it has been already demonstrated elsewhere [4] that the nontrivial solution to this equation results in  $\alpha_{\text{eq}} = 2$ , so we shall discuss only the cases (3a) and (3b). Using the explicit form of the linearized bare collision integral (10), and the explicit form of the second derivative of the entropy function, the nontrivial root of Eq. (11) is found to be

$$\alpha_{\text{eq}} = \frac{2}{K_{\text{eq}} \sum_{ij} g_i (N_i^{\text{eq}})^{-1} g_j}. \quad (12)$$

Thus, Eq. (12) together with Eq. (10) defines the linearized dressed collision integral,

$$\delta \mathbf{\Delta}^* = -2\beta \mathbf{L}^* \delta N, \quad (13)$$

where

$$L_{ij}^* = \frac{g_i(N_j^{\text{eq}})^{-1} g_j}{\sum_m g_m(N_m^{\text{eq}})^{-1} g_m}. \quad (14)$$

Now it is important to notice that operator  $L^*$  has the same *projector property* as the linearized BGK operator,

$$L^* L^* = L^*. \quad (15)$$

The image of the operator  $L^*$  is the linear subspace spanned by the vector  $\mathbf{g}$ .

With this description of the linearized dressed collision integral, we now follow the standard Chapman-Enskog analysis, and seek the solution to the kinetic equation (4) in the form,  $N = N^{\text{eq}} + \delta N^{\text{ne}}$ , where the nonequilibrium part  $\delta N^{\text{ne}}$  is orthogonal to the hydrodynamic subspace,  $(\mathbf{I}, \delta N^{\text{ne}}) = (\mathbf{c}, \delta N^{\text{ne}}) = 0$ , and is found in terms of the expansion,  $\delta N^{\text{ne}} = \epsilon \delta N^{(1)} + \epsilon^2 \delta N^{(2)} + O(\epsilon^3)$ , subject to the multiscale expansion of the time and space derivatives,  $\partial_t = \epsilon \partial_t^{(1)} + \epsilon^2 \partial_t^{(2)} + O(\epsilon^3)$ ,  $\partial_x = \epsilon \partial_x^{(1)} + O(\epsilon^2)$ . Then,

$$\begin{aligned} -2\beta \sum_j L_{ij}^* \delta N_j^{(1)} &= [\partial_t^{(1)} + c_i \partial_x] N_i^{\text{eq}}, \quad (16) \\ -2\beta \sum_j L_{ij}^* \delta N_j^{(2)} &= \partial_t^{(2)} N_i^{\text{eq}} + [\partial_t^{(1)} + c_i \partial_x] \\ &\quad \times \left[ -\beta \sum_j L_{ij}^* \delta N_j^{(1)} + \delta N_i^{(1)} \right]. \quad (17) \end{aligned}$$

By the Fredholm alternative, the solution to Eq. (16) is written

$$\delta N^{(1)} = \delta N_{\text{spec}}^{(1)} + \delta N_{\text{hom}}^{(1)},$$

where  $\delta N_{\text{hom}}^{(1)}$  is the general solution to the homogenous equation,  $L^* \delta N_{\text{hom}}^{(1)} = 0$ , and  $\delta N_{\text{spec}}^{(1)}$  is a special solution to the inhomogeneous equation (16). The homogeneous solution is equal to zero by the orthogonality condition mentioned above. The special solution has the form

$$\delta N_{\text{spec}}^{(1)} = A \mathbf{g}.$$

Thus, by the projector property (15), Eqs. (16) and (17) are equivalent to the following two equations for the special solution (we omit the subscript spec):

$$-2\beta \delta N_i^{(1)} = [\partial_t^{(1)} + c_i \partial_x] N_i^{\text{eq}}, \quad (18)$$

$$-2\beta \delta N_i^{(2)} = \partial_t^{(2)} N_i^{\text{eq}} + (1 - \beta) [\partial_t^{(1)} + c_i \partial_x] \delta N_i^{(1)}. \quad (19)$$

The latter set of equations coincides with the well known case of the LBGK, in which the BGK relaxation parameter  $\tau^{-1}$  is replaced by  $2\beta$ , and we are immediately led to the following viscosity coefficient for each of the bare collision integrals (3):

$$\nu = \frac{c_s^2(1 - \beta)}{2\beta}. \quad (20)$$

Thus, the ELBM is able to retain full control over the viscosity, while variation of the parameter  $\beta$  in the interval  $[0,1]$  covers the full linear stability interval, and the limit  $\beta \rightarrow 1$  corresponds to the zero velocity limit [4,6].

Several remarks to the derivation just given are in order: While the local equilibrium  $N^{\text{eq}}$  formally appears at the intermediate state of computation, and, in particular, in the formula for  $\alpha_{\text{eq}}$  (12), the result for the viscosity (20) is independent of it, and, in fact, the derivation has circumvented the explicit use of  $N^{\text{eq}}$ . This is a direct consequence of the projector property (15). In our example, the projector property, in turn, follows from the fact that the kinetic subspace of the model is one dimensional. Thus, all the admissible collision integrals like Eq. (3), and any others, become equivalent near the local equilibrium, and they all result in the same viscosity coefficient. This is not the case when the dimension of the kinetic subspace is larger than one. In that case, various admissible bare collision integrals may lead to different expressions for the viscosity. Nevertheless, it is always possible to construct bare collision integrals which, unlike the BGK, do not use the local equilibrium explicitly, and at the same time their linearization satisfies the projector property (15). This construction will be reported in a separate publication [14]. Finally, it should be stressed that the theoretical derivation of the viscosity coefficient is always strictly applicable only within the domain of validity of the Chapman-Enskog analysis in the vicinity of the local equilibrium.

#### IV. IMPLEMENTATION

The ELBM algorithm differs from the standard LBM in that the nonlinear equation (6) has to be solved at each time step on each lattice site. Although the time required for solving this equation does not contribute too much to the total run time, a robust algorithm is required for solving this highly nonlinear equation. Near the local equilibrium, the Newton-Raphson method fails because the first derivative tends to zero very rapidly. For this reason, we have constructed an algorithm which uses successive substitutions near the local equilibrium (if possible), and it uses a combination of the Newton-Raphson and of the bisection method [15] far away from the local equilibrium. The initial approximation, in most cases, was taken as the solution obtained from the quadratic expansion, but very far away from the local equilibrium, the solution to the equation,  $N + \alpha \Delta = 0$ ,  $\alpha > 0$ , is a better guess [6]. Details of the code are available from the authors.

#### V. SHOCK TUBE TESTS

We have studied the time evolution of a one-dimensional front in a shock tube, a very classical problem in which it appears a compressive shock front, moving in the low density, and a rarefaction front moving in the high-density region [9]. These two fronts leave an intermediate region in the central portion of the tube with uniform density  $\rho_c$ , and uniform velocity  $u_c$ . The tube is filled at time  $t=0$  with a gas at

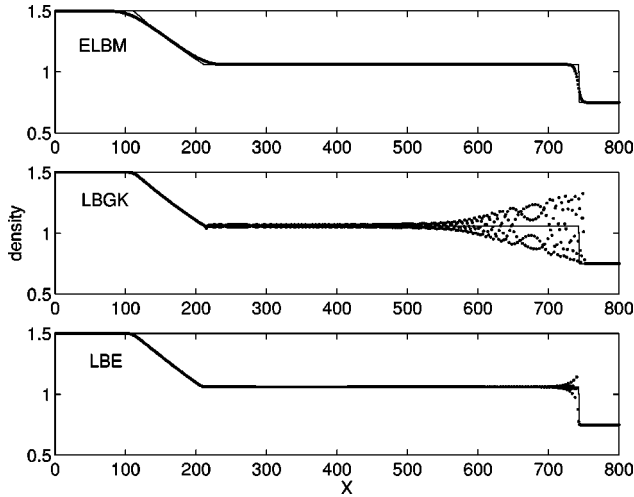


FIG. 1. Density profile (dimensionless lattice units) at  $t=500$  for viscosity  $\nu=3.3333 \times 10^{-2}$ . Thin line: Exact solution. Symbol: Simulation.

rest with uniform density  $\rho_-(u_-=0)$  for  $x<0$ , and  $\rho_+(u_+=0)$  for  $x>0$ . For the inviscid case,  $\nu=0$ , the density and velocity profiles present a discontinuity across the shock. The shock speed [9] is given by the Rankine-Hugoniot relations,

$$v_s^2 = r_c c_s^2, \quad u_c = \frac{r_c - 1}{\sqrt{r_c}} c_s, \quad r_c = \frac{\rho_c}{\rho_+}$$

and  $r_c$  can be obtained by using the Navier-Stokes relation,

$$\log r_c + \frac{r_c - 1}{\sqrt{r_c}} = \log \frac{\rho_-}{\rho_+}.$$

Simulations were performed in order to compare the stability of the three LBM algorithms: the nonlinear LBE [9] (LBE hereafter), the LBGK method with the polynomial equilibrium ansatz [13], and the present ELBM algorithm with the bare collision integral (3a).

Runs were performed on the lattice with 800 nodes. At  $t=0$  the lattice was populated as to give the density  $\rho_- = 1.5$  for  $0 \leq x \leq 400$ , and  $\rho_+ = 0.75$  for  $400 < x \leq 800$ . Standard bounce back boundary conditions were applied at both ends of the tube. Results for the three algorithms are demonstrated in Figs. 1 and 2 for a relatively high value of viscosity  $\nu=3.3333 \times 10^{-2}$ . This value was taken in order to compare all the three algorithms because it is close to the instability of the LBE [9]. It has been found that the LBGK and the ELBM never showed divergence when the viscosity was smaller than  $\nu < 10^{-3}$ . However, in contrast to the ELBM, the results of the LBGK demonstrate large fluctuations already at  $\nu < 1$ . For this reason, results of the ELBM were always better in comparison to the LBGK at low viscosity. It should be also stressed that because the theoretical derivation of the viscosity coefficient (20) is valid only in the vicinity of the local equilibrium, it may become invalid at the shocks where the populations may be far away from the local equilibrium. Increase in the effective viscosity near shocks would mean that the evaluated parameter  $\alpha$  (6) is smaller than the near-equilibrium bound (12). While we have not observed a very

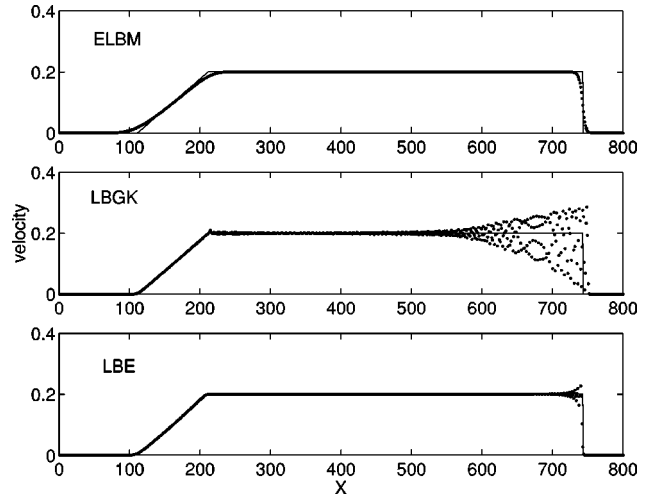


FIG. 2. Velocity profile. Simulation setup and notation same as in Fig. 1.

significant decrease of  $\alpha$  in the simulation, its deviations from Eq. (6) may explain smoothing of the density and of the velocity profiles at the shocks. On the other hand, we have not observed a development of postshock oscillations by the ELBM algorithm.

In the ELBM based on the entropy (2), the sound velocity,  $c_s = \sqrt{1/3c}$ , is not kept constant by imposing a constraint. Deviations of the effective sound velocity,

$$c'_s = [\rho^{-1} c^2 (N_-^{\text{eq}} + N_+^{\text{eq}}) - u^2],$$

from  $c_s$  measure the influence of anomalous terms [we note that these terms are of the order  $u^4$  by the choice of the entropy (2)]. The error  $E = (c'_s - c_s)/c_s$  was evaluated using the exact local equilibrium (7). In Fig. 3 the error is given for the simulation with the viscosity  $\nu=1.6 \times 10^{-13}$ . It was found that the error was of the order of 0.1% even though the Mach number was as high as 0.3464 in the present simulation.

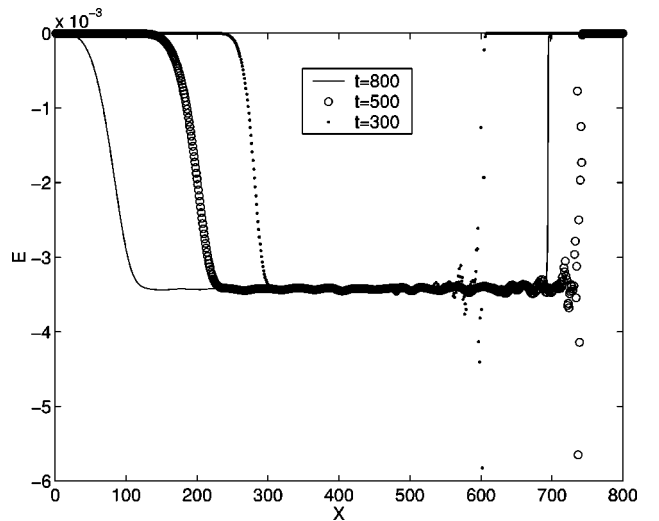


FIG. 3. Deviation of effective sound velocity from the exact sound velocity,  $E = (c'_s - c_s)/c_s$ , at  $\nu=1.6 \times 10^{-13}$ .

## VI. DISCUSSION AND CONCLUSIONS

The numerical test of the entropic lattice Boltzmann method demonstrated much better stability of this method in comparison to the LBM without the  $H$  theorem. The natural working window of this approach is low velocity ( $u \rightarrow 0$ ) and low kinematic viscosity ( $\beta \rightarrow 1$ ). Low values of velocity are required in order to keep small the anomalous terms of the order  $u^4$ , whereas the entropic estimation (6) allowed implementations very close to the zero viscosity limit.

While the entropy-based lattice Boltzmann methods are, per construction, unconditionally stable, a word of caution about their realizations is in order. On the one hand, the theoretical limit of zero kinematic viscosity is at the same time the limit of no convergence to the local equilibrium, the population vectors becomes trapped on the fixed level of the entropy function. Furthermore, implementation of the colli-

sion integrals like Eqs. (3a) or (3b) requires working with logarithmic functions which makes them more vulnerable to the round-off errors. Finally, since the whole construction is largely based on convexity of the entropy functions, and cannot tolerate any nonpositivity of the populations (unlike the standard realizations which may tolerate negative populations to some extent), care must be taken when implementing various entropy-based estimations of the collision step like Eq. (6) in order not to violate these properties. All these questions require a further detailed study, which is the subject of our current work.

## ACKNOWLEDGMENT

We thank Professor H. C. Öttinger for the encouragement and valuable discussions of results.

- 
- [1] U. Frisch, B. Hasslacher, and Y. Pomeau, *Phys. Rev. Lett.* **56**, 1505 (1986).
  - [2] Excellent reviews of the lattice Boltzmann method can be found in R. Benzi, S. Succi, and M. Vergassola, *Phys. Rep.* **222**, 147 (1992); A. J. C. Ladd, *J. Fluid Mech.* **271**, 285 (1994); Special issue on lattice gas, edited by Y. H. Qian, J. Lebowitz, and S. Orszag, *J. Stat. Phys.* **81**, 1-2, (1995); Y. H. Qian, S. Succi, and S. Orszag, *Annu. Rev. Comput. Phys.* **3**, 195 (1995); S. Chen and G. D. Doolen, *Annu. Rev. Fluid Mech.* **30**, 329 (1998).
  - [3] G. Mc Namara, G. Garcia, and B. Alder, *J. Stat. Phys.* **81**, 359 (1995).
  - [4] I. V. Karlin, A. N. Gorban, S. Succi, and V. Boffi, *Phys. Rev. Lett.* **81**, 6 (1998).
  - [5] I. V. Karlin and S. Succi, *Phys. Rev. E* **58**, 4053 (1998).
  - [6] I. V. Karlin, A. Ferrante, and H. C. Öttinger, *Europhys. Lett.* **47**, 182 (1999).
  - [7] A. Wagner, *Europhys. Lett.* **44**, 144 (1998).
  - [8] B. M. Boghosian, J. Yopez, P. V. Coveney, and A. Wagner, e-print cond-mat/0005260.
  - [9] Y. H. Qian, D. d'Humieres, and P. Lallemand, in *Advances in Kinetic Theory and Continuum Mechanics*, edited by R. Gatignol and Soubbaramayer (Springer, Berlin, 1991), p. 127.
  - [10] See, e.g., A. N. Gorban, I. V. Karlin, V. B. Zmievskii, and S. V. Dymova, *Physica A* **275**, 361 (2000), and references therein.
  - [11] M. Grmela and H. C. Öttinger, *Phys. Rev. E* **56**, 6620 (1997); H. C. Öttinger and M. Grmela, *ibid.* **56**, 6633 (1997).
  - [12] S. Chapman and T. Cowling, *The Mathematical Theory of Non-Uniform Gases* (Cambridge University Press, Cambridge, England, 1970).
  - [13] Y. H. Qian, D. d'Humières, and P. Lallemand, *Europhys. Lett.* **17**, 479 (1992).
  - [14] S. Ansumali and I. V. Karlin (unpublished).
  - [15] W. H. Press, S. A. Teukolsky, W. T. Vetterling, and B. P. Flannery, *Numerical Recipes in C* (Cambridge University Press, Cambridge, England, 1998), p. 365.